J. of Wind Eng. + Ind. Aero. Vol 21 (1985) pp 21-38.

WIND FLOW PATTERNS ABOUT BUILDINGS[a]

by J. A. Peterka,[1] M., R. N. Meroney,[2] M., and K. M. Kothari[3]

INTRODUCTION

During the past decade, much has been learned about the characteristics of flow about buildings and the structure of the wake downwind of buildings. Knowledge of building wake characteristics is useful in a variety of applications including dispersion of pollutants downwind of buildings such as conventional or nuclear power plants; airport runway interference effects; takeoff/landing limitations at heliports; pedestrian wind comfort; and wind loads on structures. Recent investigations have advanced both understanding of physical flow processes occurring in the near and far wake regions and theoretical predictive capability for flow and diffusion in the far wake region.

There is a relatively high level of misunderstanding of how wind flows around buildings, probably caused by conceptual extensions of two-dimensional flows. For example, Figure 1 shows that the separation zones for a two-dimensional obstacle are bounded by streamlines so that the separated cavities are closed. Thus pollutants released in the separated cavities can escape only by turbulent diffusion across the cavity boundary. For a three-dimensional object, the separation lines of Figure 1 are not correct as will be discussed in more

---

[a]Presented at the October 26, 1981, ASCE Convention and Exposition held in St. Louis, Missouri.

[1]Assoc. Professor, Fluid Mechanics and Wind Engineering Program, Dept. of Civil Engrg., Colorado State Univ., Fort Collins, CO.

[2]Professor, Fluid Mechanics and Wind Engineering Program, Dept. Civil Engrg., Colorado State Univ., Fort Collins, CO.

[3]Asst. Res. Professor, Fluid Mechanics and Wind Engineering Program, Dept. Civil Engrg., Colorado State Univ., Fort Collins, CO.

CEP81-82JAP-RNM-KMK12

detail below, and pollutants may enter or escape the separation cavity by convection. Some prediction formulae incorrectly assume pollutants can enter the three-dimensional separation cavity only by turbulent diffusion across this cavity boundary.

NEAR-FIELD FLOW

Very little data defining the flow field about buildings is available from full-scale tests: Colmer [1] and Frost and Shahabi [2] reported limited measurements of mean velocity and turbulence intensity downwind of buildings from which decay of velocity defect with distance downwind could be determined. Other full-scale measurements related to pedestrian comfort have reported velocities at isolated points near buildings, but not in a way which would contribute significantly to an understanding of the flow characteristics about buildings.

Much of the current knowledge relating to three-dimensional wind flows around buildings has been obtained by means of model tests in boundary-layer wind tunnels. Important publications based on such wind-tunnel tests are: Counihan [3], Lemberg [4], Peterka and Cermak [5], Hansen and Cermak [6], Castro and Robins [7], Woo, Peterka and Cermak [8], Hunt, Abell, Peterka and Woo [9], Kothari, Peterka and Meroney [10], and others too numerous to include in this brief review. An excellent review including more details related to diffusion is presented by Hosker [11]. These studies showed that three-dimensional obstacles cause fundamental differences in flow characteristics from those originated by two-dimensional obstacles. Oil flow studies [8,9], see Figure 2, permitted an identification of mean surface-shear-stress patterns on both the ground plane and on the building surface. In combination with smoke flow studies and

kinematic analysis, these data provided the basis for the mean flow patterns which are shown in Figures 3-5 based on references [8,9].

Figure 3 shows that the mean streamlines for flow about a single building form a complex flow geometry. The flow approaching the obstacle separates from the surface a distance upwind of the building. This separation location is dependent to the first order on building height-to-width ratio, building height-to-boundary-layer-height ratio and upstream surface roughness. The vorticity in this separated flow, in combination with the pressure distribution on the front of the building, results in downward flow on the front of the building. This subsequently causes the separated flow to roll up into a vortex. The vortex is wrapped around the building by convection into a horseshoe shape. The primary vortex induces additional vortices of smaller size and strength, Figures 3 and 4, which are eventually incorporated into the primary vortex around the side of the building and lose their individual identity. The horseshoe vortex can be identified in the flow at some distance downwind.

The wind that impinges on the front of the building forms a stagnation region between 2/3 and 3/4 of the building height depending on building height-to-width ratio. From this region, flow moves outward toward all front edges of the building. The flow separates at the front edge of the top and sides and may or may not reattach to the top or sides before reaching the back edges. Reattachment depends on building length-to-width ratio, height-to-length ratio and upstream roughness (which determines the turbulence intensity in the approaching wind--a significant factor in distance to reattachment). Figures 3 and 4 show

flow patterns for a reattached flow; Figure 5 shows flow patterns for an unreattached flow.

A separation cavity covers the rear face of the building and also the top and sides when reattachment on the sides does not occur. Examination of Figures 3-5 reveals that the mean streamline reattaching to the ground surface downwind of the building originates in the flow upwind of the building and not at a separation point on the building. The same is true of the streamline which forms a stagnation point on the rear face. Thus the mean flow field convects mass directly into the separation cavity, and, by continuity of mass, it also convects flow out of the cavity region. The direct convection out is more difficult to visualize but involves off-centerline flow departing from the two standing vortices with vertical axes forming an arch at the back corner and probably entrainment into the horseshoe vortex. For this reason, transport of pollutants into or out of the separation cavity is primarily accomplished by convection and not by turbulent dispersion. If the cavity length is defined by the centerline reattachment point downwind of the body, then the cavity length can vary from 2-6 or more building heights [11]. Because of the direct convection into and out of the cavity, a precise definition of cavity boundary may not be meaningful.

The organized picture of the cavity described above is made cloudy by the existence of a high level of turbulence in this region. Smoke flow and bubble track experiments suggest that the separation cavity is completely "washed out" by turbulent gusts at times. Thus the use at this time of the mean streamline model described above for more than a qualitative understanding of the flow field must be approached with

caution. Some quantification of the mean flow field has begun with velocity-measuring devices capable of correctly evaluating the effects of high turbulence levels and reverse flows, see Davies, Quincey and Tindall [12].

The flow field described in Figure 3 has significant implications for pedestrians and for dispersion of pollutants about the building. For example, the wind flows downward on the front face of the building from the front stagnation region and around the corner of the building at the base as it wraps up into the horseshoe vortex. This effectively brings velocity magnitudes associated with approach wind velocities at about 3/4 the height of the building to the surface at the front corners of the buildings. Immediately around the corner at the ground level in the separated flow zone, the velocities are quite low. Most city pedestrians who have walked around the corner of a tall building into a blast of wind are familiar with this phenomena, if not its cause. The addition of nearby buildings can, in some cases, increase this velocity. The high turbulence levels associated with the separated zones can cause a decrease in control for helicopters which might try to land on the roof or ground. Pollutants from roof exhausts can become entrained in flows which recirculate to the back and sides of the building where ventilation intakes are frequently located; see, for example, Li and Meroney [13]. A significant amount of indoor air pollution and cooling tower recirculation can be attributed to the circulations within separated flow zones about buildings.

FAR-FIELD FLOW

The reattached flow downstream from the building requires some distance before the wind recovers the characteristics of the approach

boundary layer and all disturbances caused by the building disappear. This wake region is characterized when compared to the approaching wind flow by a lower mean velocity, higher turbulence intensity, smaller scales of turbulence and, in some cases, organized vorticity with its axis parallel to the wind direction. Figure 6 defines several variables used below.

Figure 7 shows the distribution of velocity defect (defined as the difference between upstream approach velocity at height z and the local mean velocity at height z) on the building centerline downwind of a building from reference [5] with $H/\delta = 0.11$, $H/W = 0.4$, $W/D = 3.25$, $\alpha = 0°$. The maximum velocity defect gradually decreases but is still detectable at $x/H = 18$ for this combination of building and approach flow characteristics (power law exponent = 0.24). A slight increase in velocity is noted just above the separated shear layer forming the top edge of the cavity for $x/H = 0.5$ to 2. The wake height increases monotonically with distance downwind to a height of 3-4H.

Figure 8, from reference [5], shows the distribution of mean velocity in the horizontal direction perpendicular to the approach velocity at a height of $z/H = 0.8$. The same characteristics can be observed which were noted for Figure 7--a gradual decrease in magnitude of velocity defect, an accelerated flow near the separated shear layer and a monotonically increasing wake width to about 4 W/2 (4 half-widths of the building from the centerline). A secondary maximum in the velocity defect profile can be noted when x/H is from 2 to 12 near $y/(W/2) = 2$ to 2.5. This is the result of the horseshoe vortex which convects lower momentum fluid upward in the boundary layer at the

region of the secondary maxima increasing the velocity defect. The vortex also convects higher momentum fluid downward in the region between the maxima near $y/(W/2) = 1$ to 1.5 resulting in a smaller velocity defect at that location.

The wake characteristics of Figures 7 and 8 are not universal for all building aspect ratios or approach roughness conditions. A rougher boundary upwind of the building results in a higher level of turbulence in the approach wind causing the wake to disappear more quickly and evidence of the horseshoe vortex in the wake to diminish. A smoother approach boundary causes the wake to be detectable to a greater downwind distance and the horseshoe vortex to remain in evidence longer.

The influence of building aspect ratio on magnitude and persistence of the wake is presented in Figure 9, modified from reference [5], in which the largest velocity defect at any downstream distance is plotted against distance downwind. The model data were acquired in a 0.24 power law boundary layer. Field data from Colmer [1] and Frost et al. [2] are plotted with the wind-tunnel data. For practical purposes, the extent of the wake in a suburban setting is 3 to 6 building heights for buildings with width 1/3 or 1/4 their height and is 10 to 30 building heights for buildings whose width is 1 to 4 times their height. The Colmer data may not have been obtained on the wake centerline. This would result in an underestimation of the wake defect.

One characteristic of building wakes is usually a substantial increase in turbulence in the wake, accompanied by a shift in turbulent energy to smaller scales. Figure 10 shows the decay of turbulence downstream from the model buildings whose mean velocity defects were plotted in Figure 9. The effective length of the turbulence wakes was about the

same as for the mean velocity wake. The turbulence increase in the wake downstream is significantly reduced when the vortex wake is stronger--for example in the wake of a hemisphere [6] or in stably stratified flow [10]. In this case high-momentum, low-turbulence flow from above the hemisphere is brought down close to the ground on the wake centerline by the vortex pair and results in a mean velocity excess and a turbulence defect.

A rectangular building can produce vorticity in the wake with axis parallel to the approach flow direction by mechanisms other than those associated with the horseshoe vortex. With a building rotated so that one side is approximately 45 degrees to the approach flow, a pair of rooftop vortices forms over the upwind corner whose axes can become aligned with the flow in the wake. When one of these vortices is much stronger than the other, its presence in the wake can dramatically extend the length of the wake. Figure 11, from [14], shows the mean velocity defect downwind of a building whose side ratio is 2.6. A mean velocity excess remained at a significant magnitude 80 building heights downwind where wind-tunnel test-section length limitations prevented further measurements.

THEORETICAL PREDICTIONS

Despite the considerable complexity of the flow around and downstream of a building, a reasonably simple but effective analysis is possible to provide quantitative predictions of wake behavior. In 1969, Hunt and Smith [15] published a momentum wake theory for the mean velocity defect in the wake of a three-dimensional obstacle immersed within a turbulent boundary-layer flow. Momentum wake theory is based on the assumptions that only small perturbations to the turbulent boundary layer are caused by the obstacle, that the ratio of the model height to the boundary-layer

height is very small, that the velocity profile power-law exponent is small, and that the mixing may be represented by a constant eddy viscosity. This theory is valid only for the far-wake region because the separated region behind the building cannot be considered to be a small perturbation on the approach flow. The mean velocity defect predicted from the three-dimensional momentum-wake theory can be expressed as (see Figure 6 for coordinates and wake schematic):

$$\frac{u(x, y, z)}{U_H} = k_1 F_1(z'', y'')/[(x - a)/H]^{\frac{3+n}{2+n}}, \qquad (1)$$

where $u(x, y, z)$ = velocity defect,

U_H = approach velocity at building height H,

a = virtual origin of the wake,

n = velocity profile power-law exponent,

$$k_1 = 0.21\, C_{Fx}(W/H)/\left\{4\lambda^{1/2}\gamma(2K^2n/(2+n))^{\frac{3+n}{2+n}}\right\},$$

W = width of building,

λ and γ = constants of order one,

K = von Karman constant (0.41),

C_{Fx} = force coefficient of building,

$$F_1(z'', y'') = \frac{\eta^{\frac{1}{2+n}}\,\mathrm{Exp}[-(\eta + y''^2/(1.5 + \eta))]}{(\eta + 1.5)^{1/2}}$$

$$z'' = (z/H)/[(x - a)/H]^{\frac{1}{2+n}},$$

$$\eta = z''^{(2+n)}/[2(2 + n)K^2n\gamma],$$

$$y'' = \frac{(y/H)}{[(x - a)/H]^{\frac{1}{(2+n)}}}\left[\frac{2 + n}{2\lambda\gamma K^2 n}\right]^{\frac{1}{(2+n)}}.$$

Thus, for the wake of a three-dimensional building and small n, the theory predicts that the mean velocity defect decays as $x^{-1.5}$. A similar prediction for the turbulent intensity excess decay rate suggests proportionality to x^{-2} (Hunt [16]).

Measurements of Peterka and Cermak [5] did not confirm the existence of a Gaussian distribution of velocity defect in the crosswind direction incorporated in the momentum wake theory. They concluded that this effect was the result of the horseshoe vortex which forms in the stagnation region at the front of the building and wraps around the building to produce a mean vorticity with the axis in the longitudinal direction. Noting this result, Hunt [17] subsequently developed a vortex-wake theory to account for these vortices. The longitudinal velocity excess in the inviscid zone was determined by Hunt [17] and given by,

$$u = \frac{n\Gamma hy'x}{\pi}\left[\frac{1}{(y'^2 + h^2 + z^2)^2 - 4z^2h^2}\right], \qquad (2)$$

where $y' = y_v - y$. y_v and h are the distances to the center of the imposed vortex in the lateral and vertical directions, respectively, and Γ is the circulation at $x = 0$.

The physics of vortex and momentum wake mechanisms were applied to any passive scalar such as temperature by Kothari, Peterka and Meroney [10]. They developed the theory to predict the time mean temperature field behind a three-dimensional bluff body immersed deeply in a turbulent stably stratified boundary layer. Some of the results for the velocity field from Hunt's vortex wake theory [17] were used to derive the model for the temperature field.

Transport of the scalar quantity temperature is governed by the energy equation. With the assumptions that only small perturbations

to the thermal boundary layer are caused by an obstacle, that the ratio of the model height to the boundary-layer height (velocity or temperature) is very small, that the velocity and temperature power-law exponents are small, that the dissipation and molecular diffusivity are small, and that the mixing may be represented by a constant eddy diffusivity, Kothari, Peterka and Meroney [10] obtained the temperature perturbation induced by the obstacle on the approach thermal boundary layer. The three-dimensional temperature perturbation solution for a flow field subjected to only momentum-wake effects is given by:

$$\frac{\theta(x,y,z)}{\text{DELTA T}} = k_2 \frac{T_H}{\text{DELTA T}} \frac{F_2(z'',\, y'')}{\left(\frac{x - a}{H}\right)^{\frac{3+n}{2+n}}}, \tag{3}$$

where DELTA T $= T_\delta - T_{z_1}$ in the undisturbed boundary layer,

T_δ = mean temperature at the top of the turbulent boundary layer,

T_{z_1} = mean temperature at a reference height z_1,

T_H = mean temperature at height H in the approach flow,

k_2 = constant determined from experiment,

a = virtual origin of the wake,

n = velocity profile power-law exponent,

$$F_2(z'',y'') = \frac{\eta^{\frac{1}{2+n}}}{(\eta + 1.5)^{1/2}} \text{Exp}\left[-\left(\eta + c_8 \frac{y''^2}{(\eta + 1.5)}\right)\right],$$

$$z'' = \frac{(z/H)}{\left[\frac{x - a}{H}\right]^{\frac{1}{(2+n)}}},$$

$$\eta = \frac{z''^{(2+n)}}{[2(2 + n)K^2 n\, 0.85\gamma]},$$

$$y'' = \frac{(y/H)}{\left[\frac{x - a}{H}\right]^{\frac{1}{(2+n)}}} \left(\frac{(2 + n)}{2\lambda\, 0.85\, \gamma K^2 n} \right)^{\frac{1}{(2+n)}}$$

K = von Karman constant (0.41),

c_8 = constant--not needed on $y = 0$.

The excess temperature induced by the trailing horseshoe vortices was also determined by Kothari et al. [10] and is given by

$$\theta = \frac{n\Gamma h y' x}{\pi} \left[\frac{1}{(y'^2 + h^2 + z^2)^2 - 4z^2h^2} \right] \frac{T_H}{U_H} \qquad (4)$$

To consider the effect of two horshoe vortices along the centerline of a building the perturbation effects of the vortices must be doubled in the calculation. The total velocity defect and temperature excess are given by the algebraic sum of equation (1) and twice equation (2) and by the algebraic sum of equation (3) and twice equation (4), respectively.

COMPARISON OF MEASUREMENTS WITH THEORIES

The theories of Hunt [15,17] and Kothari, Peterka and Meroney [10] for the mean velocity and temperature for momentum and vortex wakes behind the building are evaluated in this section. The experimental data of Peterka and Cermak [5] and Kothari et al. [10] have been utilized for comparison with the theories.

The momentum theory requires knowledge of the force coefficient, C_{Fx}, on the building which was derived from data in Akins et al. [18]. The constants λ and γ were assumed equal to one. The virtual origins for the buildings were derived from the technique suggested by Hunt [16].

From the momentum wake theory, equation (1), it can be shown that the maximum velocity defect occurs on the wake centerline at

$$\frac{z}{H} \simeq 0.26 \left(\frac{x - a}{H}\right)^{\frac{1}{(2+n)}} \tag{5}$$

The maximum velocity defect from equation (1) at this height for small n and large x is:

$$\frac{u}{U_H} \propto \frac{W}{H} \left(\frac{x}{H}\right)^{-3/2} = \left[\frac{x}{H} \left(\frac{H}{W}\right)^{2/3}\right]^{-3/2} . \tag{6}$$

The constant of proportionality can be obtained by evaluation of equation (1). The authors have found that an additional factor to account for initial vertical mixing in the near wake improves the correlation of data obtained behind rectangular buildings:

$$\frac{u}{U_H} = f\left[\frac{x}{H} \left(\frac{H}{W}\right)^{2/3} \left(\frac{H}{\delta}\right)^{2n}\right] \tag{7}$$

Data from Figure 9 are plotted in Figure 12 using variables defined by equation (7). Also plotted in the same variables is the range of maximum velocity defects predicted by equation (1) using (5) and $C_{Fx} = 1.2$, $\gamma = \lambda = 1$, $n = 0.2$ and $a = -2H$. The data collapse well but fall under the momentum wake predictions. The difference between prediction and data may be due to vortex wake effects which could be predicted using equation (2) or due to initial vertical mixing in the near wake not included explicitly in the theory. Application of equation (2) did not give a consistent improvement for all cases. Until further study is completed, a reasonable approximation of peak momentum defect for rectangular buildings is:

$$\frac{u}{U_H} = 0.16 \left[\frac{x}{H} \left(\frac{H}{W}\right)^{2/3} \left(\frac{H}{\delta}\right)^{2n}\right]^{-1.3}$$

in which a constant full-scale value of $\delta = 1000$ ft can be used without significant impact on the answer computed.

The data of Kothari et al. [10] in a stably stratified flow showed indications that the horseshoe vortex was an important factor in the wake structure. Figures 13 and 14, from [10], show the comparison of analytical and experimental vertical profiles of mean velocity and temperature on the wake centerline. The calculations of momentum and vortex wake effects were made using the theories discussed above. The vortex location was estimated from data in reference [6] while vortex strength was estimated by a procedure developed in reference [10]. The effect of the momentum wake is to decrease velocity and decrease temperature while the effect of the vortex wake is to increase velocity and temperature by pulling high momentum, high temperature fluid down into the wake. As shown in Figures 13 and 14, the sum of the momentum and vortex wake effects matches the data well. One constant in the temperature theory, k_2, was not available through the theory and had to be set by comparison with data. The value of k_2 was selected to force a match between theory and experiment at $x/H = 10$ and $z = 1$. Additional research is needed to determine a method for predicting k_2 without data. No free constants were needed for the velocity comparisons. The comparison between theory and experiment is excellent except in the near wake where the perturbations are large and the theory should not be valid. Note that the vortex is sufficiently strong in this weakly stably stratified flow that a velocity excess and temperature increase are produced in the wake. The momentum wake theory alone cannot adequately model such a wake.

CONCENTRATION PREDICTION

A theory for dispersion of pollutants in the wake has been developed [19] in a manner parallel to that for temperature discussed

above. Application of this theory to dispersion in the wake of nuclear power plants has been made [20,21]. Figure 15 from reference [20] shows a comparison of largest mean concentration in the wake of a power plant and the prediction. One free coefficient appears in the theory. Comparisons between theory and experiment to date are encouraging and are the subject of continuing research.

CONCLUSION

On the basis of research conducted during the last decade investigating wind flow around and downwind of buildings, several conclusions are evident:

1. Wind flow about three-dimensional buildings results in separated flow regions fundamentally different from those about two-dimensional buildings. Fluid is convected into and out of separated zones for the three-dimensional case while turbulent diffusion is the primary mode of fluid exchange for the two-dimensional case.

2. Mean streamline patterns for flow about buildings have been proposed which provide a basis for further research into wind magnitudes and dispersal patterns near buildings.

3. Analytical methods have been developed which provide an effective prediction of mean velocity, turbulence intensity, mean temperature and mean concentration of pollutants in the wake region downwind of buildings. Additional research is needed to further refine these methods.

ACKNOWLEDGEMENTS

The writers are indebted to the Nuclear Regulatory Commission, the Electric Power Research Institute and the National Aeronautics and Space Administration for support which has led to many of the results discussed in this paper.

Appendix I--References

1. Colmer, M. J., "Some Full-Scale Measurements of the Flow in the Wake of a Hanger," ARC-CP-1166, 1971.

2. Frost, W. and Shahabi, A. M., "A Field Study of Wind over a Simulated Block Building," NASA Report CR-2804, 1977.

3. Counihan, J., "An Experimental Investigation of the Wake behind a Two-Dimensional Block and behind a Cube in a Simulated Boundary Layer Flow," CERL Lab. Note: RD/L/N115/71, 1971.

4. Lemberg, R., "On the Wakes behind Bluff Bodies in a Turbulent Boundary Layer," University of Western Ontario Report BLWT-3-73, 1973.

5. Peterka, J. A. and Cermak, J. E., "Turbulence in Building Wakes," Fourth International Conference on Wind Effects on Buildings and Structures, London, pp. 447-463, September 1975.

6. Hansen, A. C. and Cermak, J. E., "Vortex-Containing Wakes of Surface Obstacles," Fluid Dynamics and Diffusion Laboratory Report CER75-76ACH-JEC16, Colorado State University, Fort Collins, Colorado, 1975.

7. Castro, I. P. and Robins, A. G., "The Effect of a Thick Incident Boundary Layer on the Flow around a Small Surface Mounted Cube," Central Electricity Generating Board Report R/M/N795, 1975.

8. Woo, H. G. C., Peterka, J. A., and Cermak, J. E., "Wind-Tunnel Measurements in the Wakes of Structures," NASA Contractor Report NASA CR-2806, 1977.

9. Hunt, J. C. R., Abell, C. J., Peterka, J. A., and Woo, H., "Kinematical Studies of the Flows around Free or Surface-Mounted Obstacles; Applying Topology to Flow Visualization," Journal of Fluid Mechanics, Vol. 86, Part 1, pp. 179-200, 1978.

10. Kothari, K. M., Peterka, J. A., and Meroney, R. N., "Stably Stratified Building Wakes," U.S. NRC Report NUREG/CR-1247, 1979.

11. Hosker, R. P., "Flow and Diffusion near Obstacles," Chapter 7 in Atmospheric Science and Power Production, D. Randerson, editor, (U.S. Department of Energy), in publication.

12. Davies, M. E., Quincey, V. G., and Tindall, S. J., "The Near-Wake of a Tall Building Block in Uniform and Turbulent Flows," Wind Engineering, Proceedings of the Fifth International Conference, Fort Collins, Colorado, J. E. Cermak, ed., pp. 289-298, 1979.

13. Li, W. W. and Meroney, R. N., "Gas Dispersion near Cubical Model Buildings, Part I: Mean Concentration Measurements," submitted to Journal of Wind Engineering and Industrial Aerodynamics, 1981.

14. Hansen, A. C., Peterka, J. A., and Cermak, J. E., "Wind-Tunnel Measurements in the Wake of a Simple Structure in a Simulated Atmospheric Flow," NASA Contractor Report NASA-CR-2450, 1975.

15. Hunt, J. C. R. and Smith, J. P., "A Theory of Wakes behind Buildings and Some Provisional Experimental Results," Central Electricity Research Laboratory Report RD/L/N31/69, 1969.

16. Hunt, J. C. R., "Further Aspects of the Theory of Wakes behind Buildings and Comparison of Theory with Experiment," Central Electricity Research Laboratory Report RD/L/R/1665, 1971.

17. Hunt, J. C. R., "Vortex and Momentum Wakes behind Surface Obstacles in Turbulent Boundary Layers," to be published.

18. Akins, R. E., Peterka, J. A., and Cermak, J. E., "Mean Force and Moment Coefficients for Buildings in Turbulent Boundary Layers," Journal of Industrial Aerodynamics, Vol. 2, pp. 195-209, 1977.

19. Kothari, K. M., Peterka, J. A., and Meroney, R. N., "An Analytical Method for Determination of Dispersion in the Wake of a Power Plant," to be published.

20. Kothari, K. M., Peterka, J. A., and Meroney, R. N., "The Wake and Diffusion Structure behind a Model Industrial Complex," Nuclear Regulatory report NUREG/CR-1473, 1981.

21. Kothari, K. M., Meroney, R. N., and Peterka, J. A., "Nuclear Power Plant Building Wake Effects on Atmospheric Diffusion: Simulation in Wind Tunnel," Electric Power Research Institute report EPRI NP-1891, 1981.

Appendix II--Notation

A	reference area for concentration measurements
a	virtual origin of wake
C_{Fx}	force coefficient of building in x direction
C_w	wake concentration of pollutant
H	building height
h	vertical height of center of vortex
K	von Karman constant
k_2	constant
n	mean velocity power law exponent
Q	pollutant source strength
T	mean fluid temperature
T_H	mean temperature at height H in approach flow
T_{z_1}	mean temperature at the height z_1
U	mean velocity in x direction
U_H	approach mean velocity at height H
U_δ	approach mean velocity at height δ
u	mean velocity defect in wake (U(z) approach-U(z) wake)
x, y, z	space coordinates, x downwind, y lateral, z vertical
y_v	lateral distance to center of vortex

Greek Symbols

α	approach wind direction
Γ	circulation of vortex at $x = 0$
δ	boundary-layer thickness
θ	mean temperature excess in wake (T(z) wake-T(z) approach)
γ, λ	constant of order one

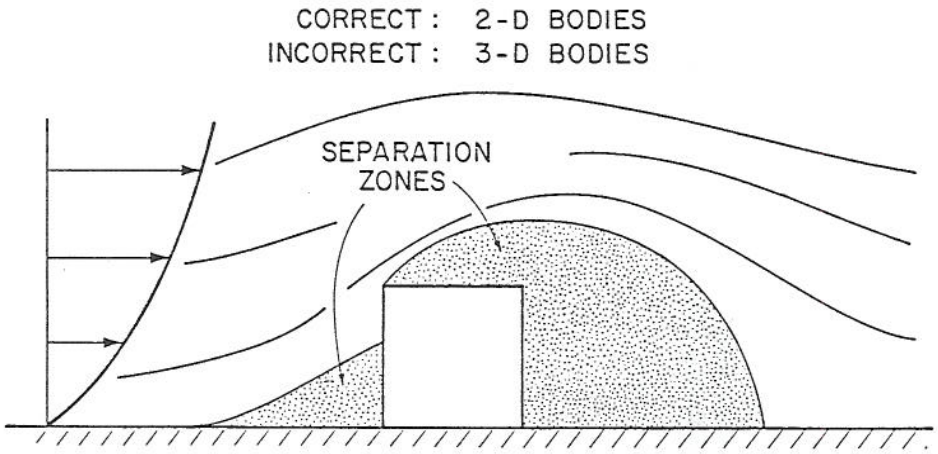

Figure 1. Separation cavities for two-dimensional flow.

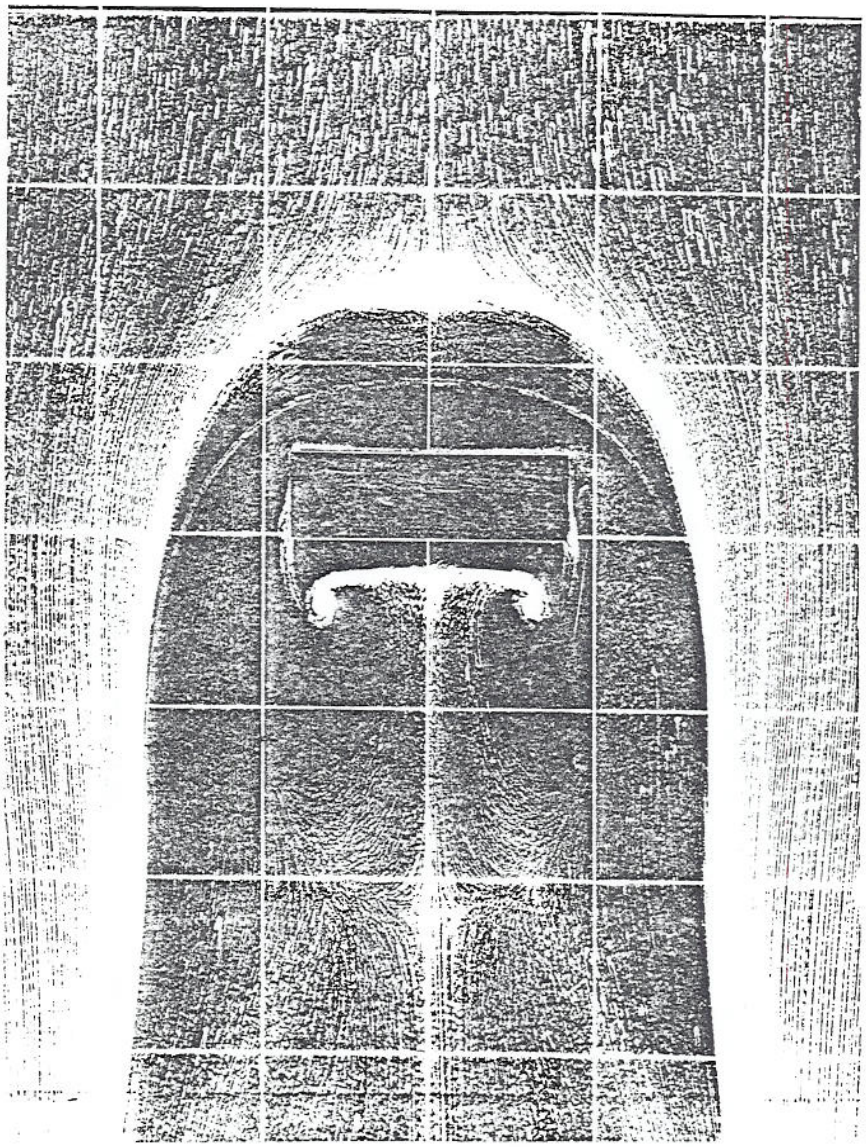

Figure 2. Surface shear-stress patterns, refs. [8,9].

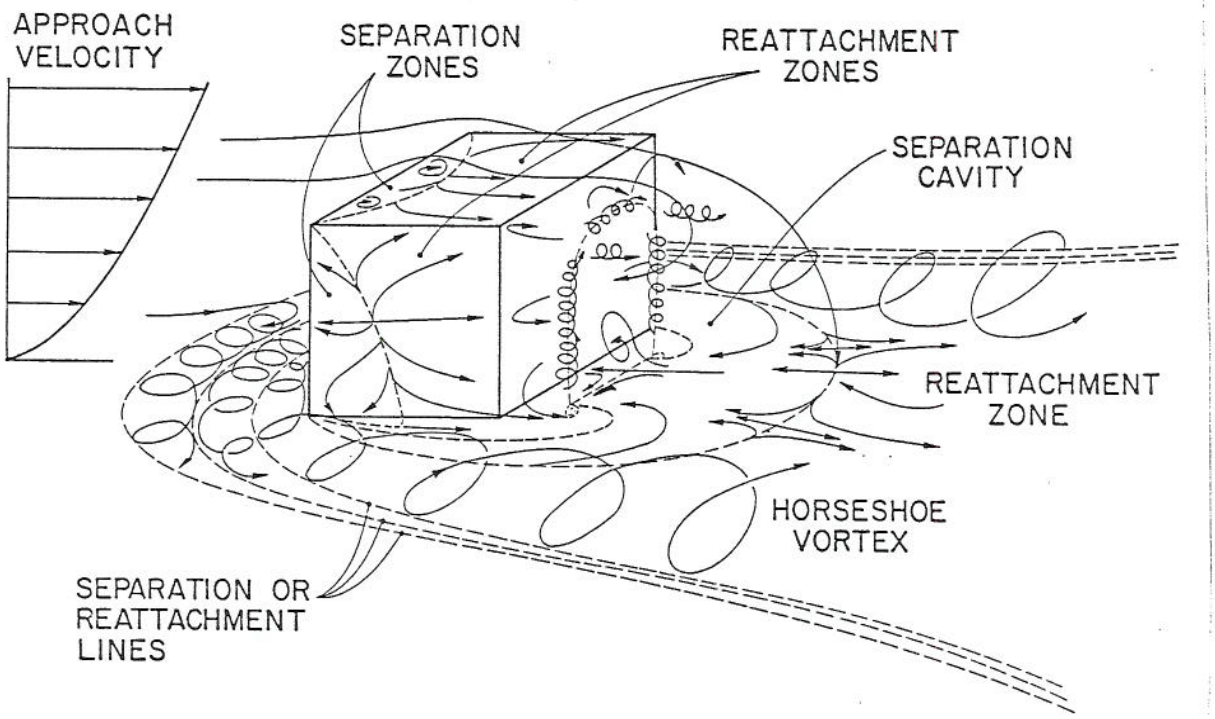

Figure 3. Mean streamline patterns about a building, refs. [8,9].

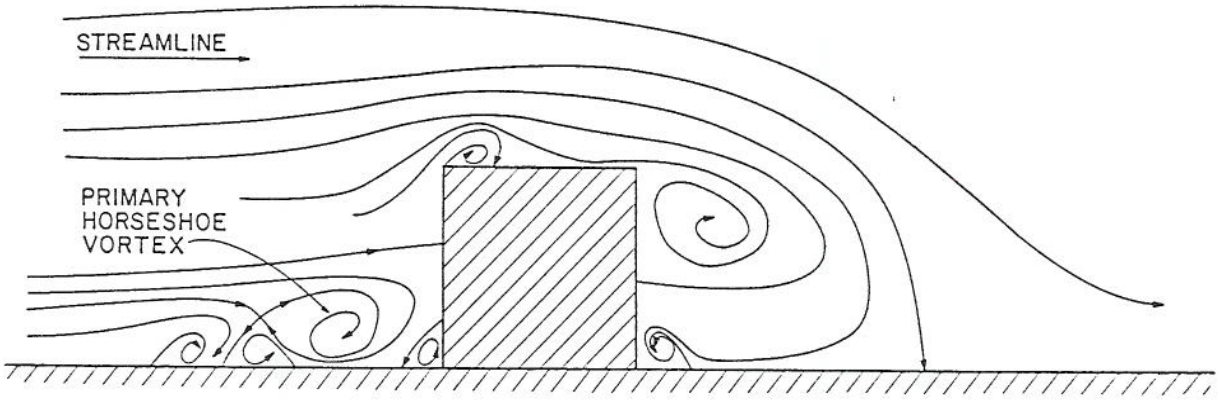

Figure 4. Centerline streamline patterns for flow reattaching to top, ref. [9].

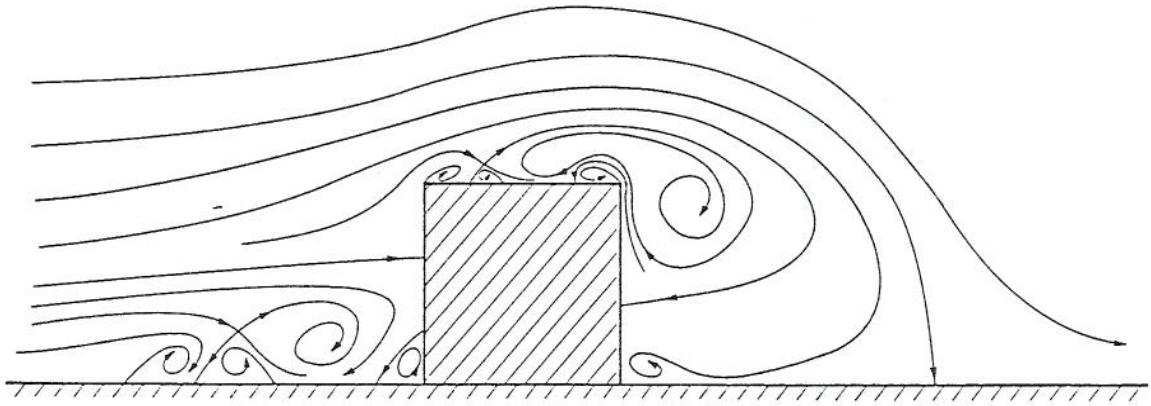

Figure 5. Centerline streamline patterns for flow not reattaching to top, ref. [9].

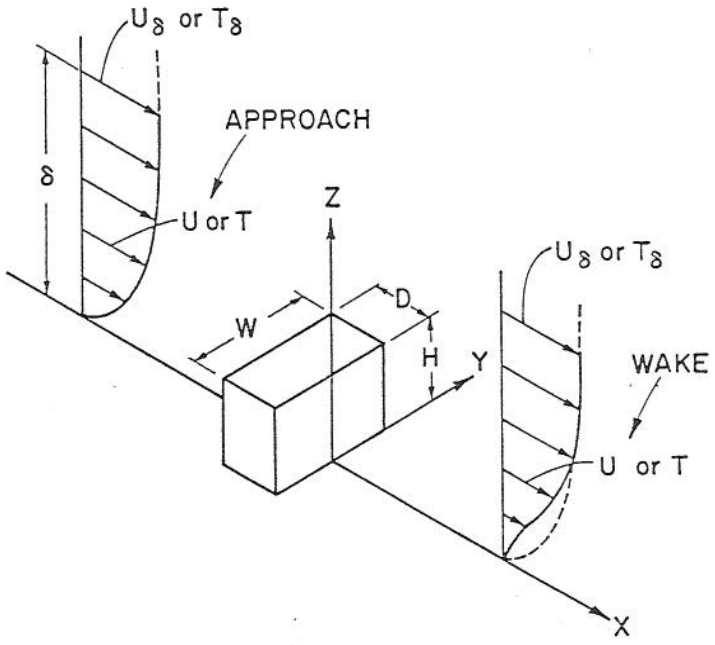

Figure 6. Definition of variables.

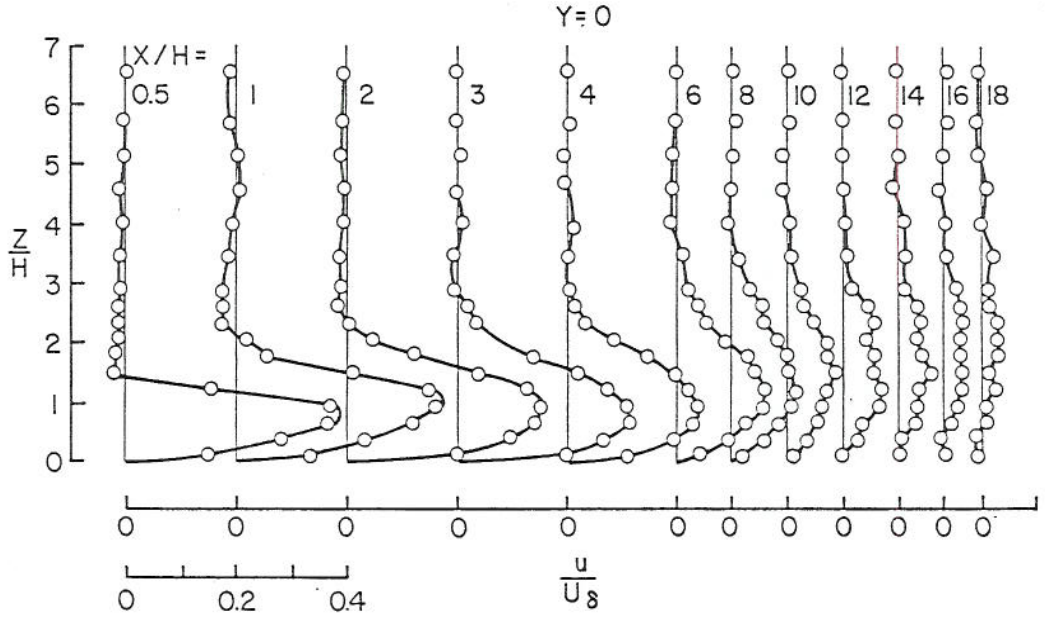

Figure 7. Vertical profiles of mean velocity defect on wake centerline, ref. [5].

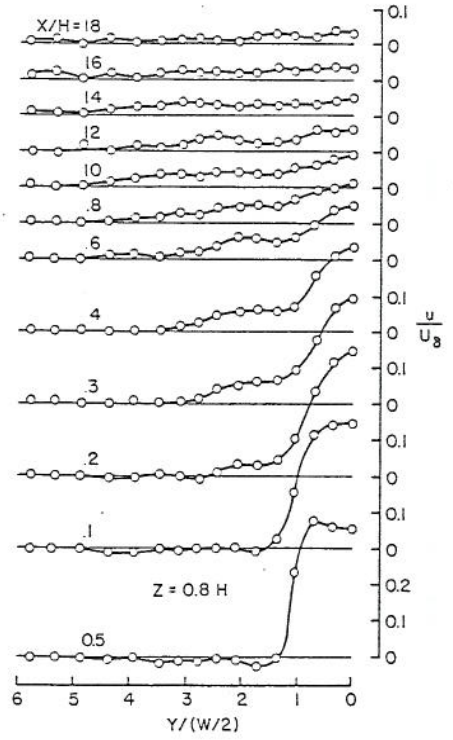

Figure 8. Horizontal profiles of mean velocity defect in wake, ref. [5].

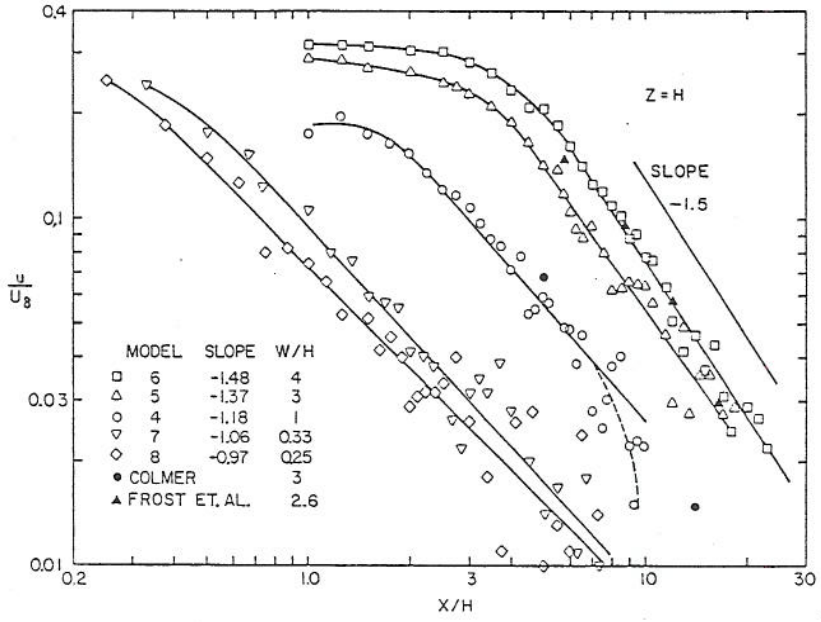

Figure 9. Maximum mean velocity defects in the wakes of several buildings, ref. [5].

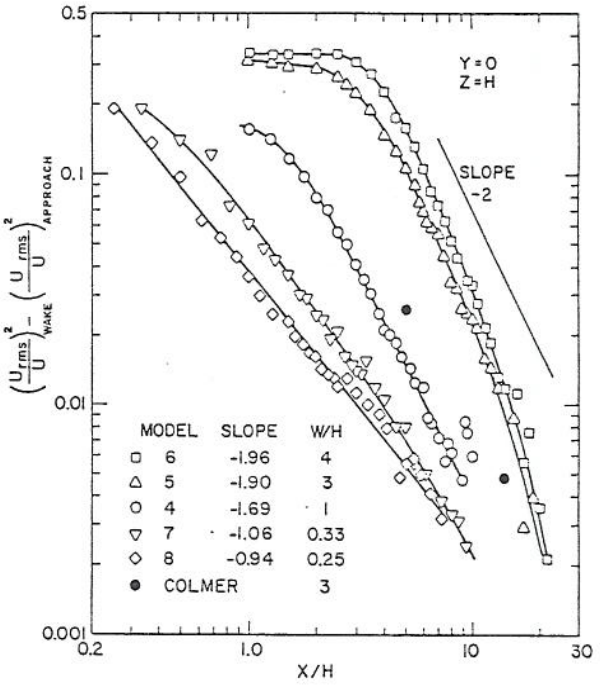

Figure 10. Maximum turbulence intensity excess in the wakes of several buildings.

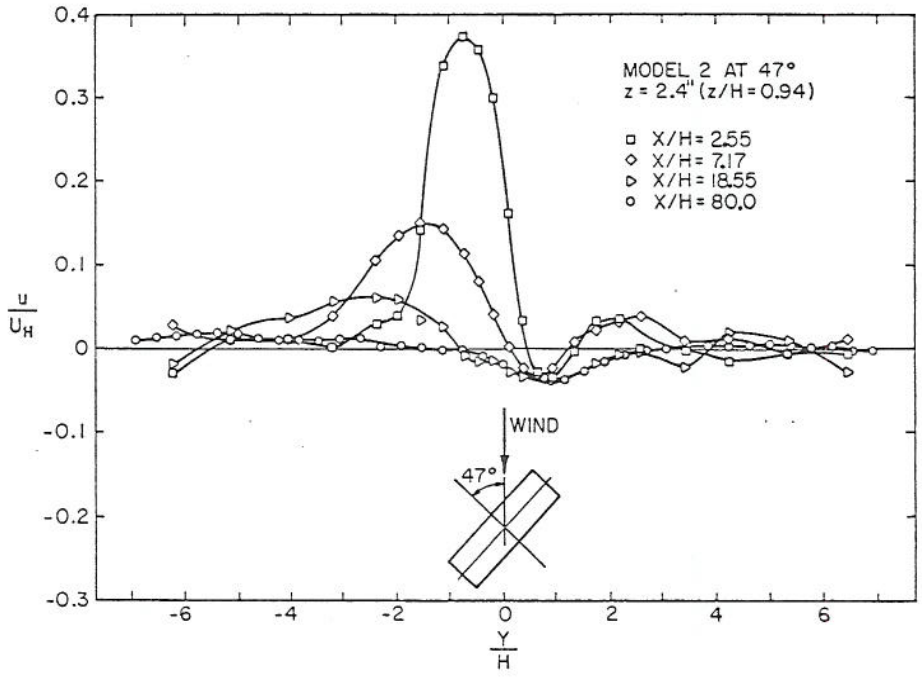

Figure 11. Horizontal profiles of velocity defect in the wake of a building at angle to the flow, ref. [14].

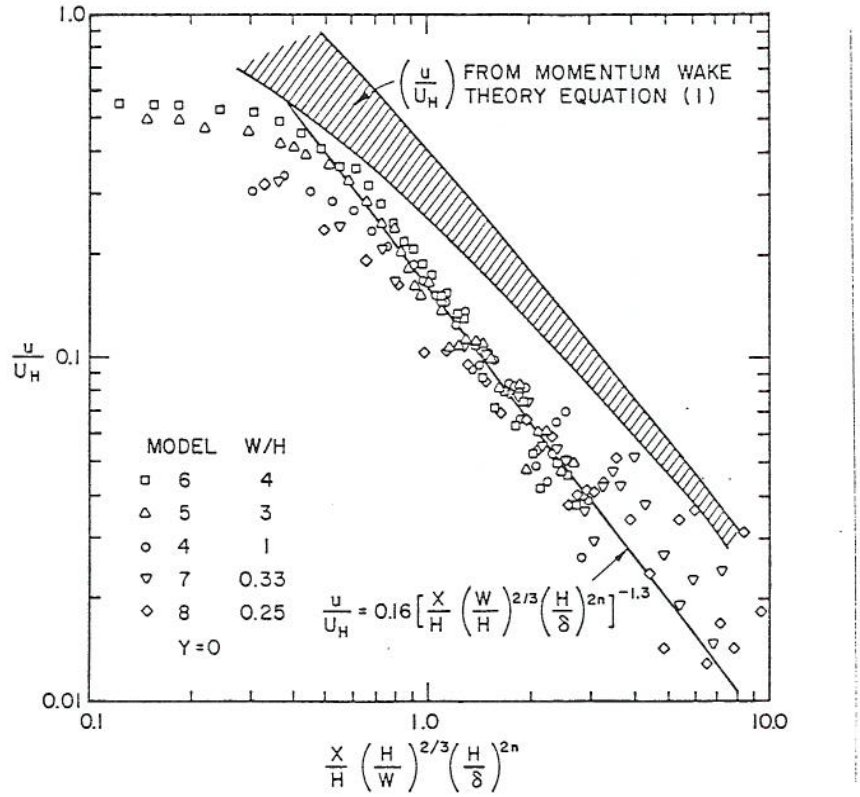

Figure 12. Comparison of maximum momentum defect with theory.

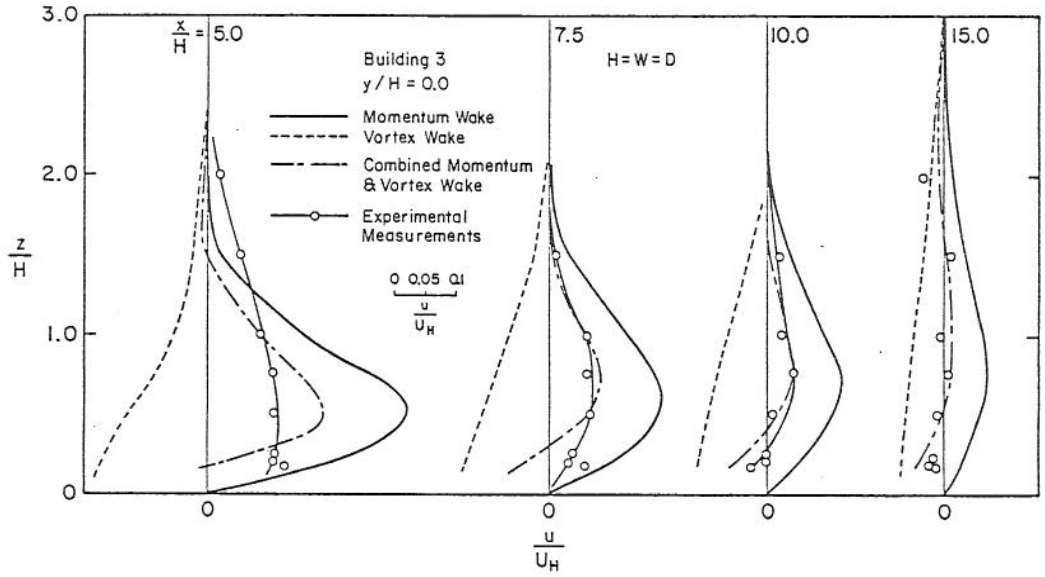

Figure 13. Comparison of vertical profiles of velocity defect on wake centerline in stably stratified flow with theory, ref. [10].

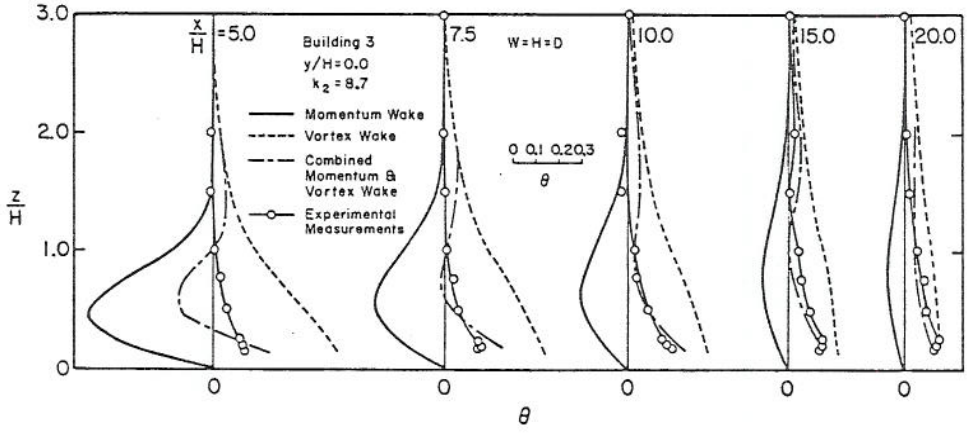

Figure 14. Comparison of vertical profiles of temperature excess on wake centerline in stably stratified flow with theory, ref. [10].

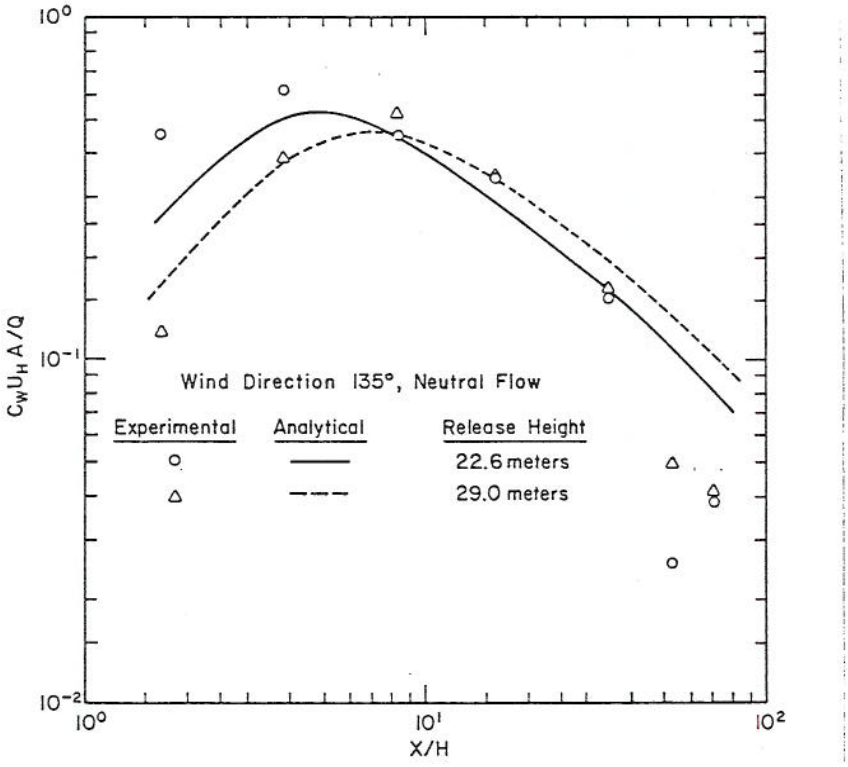

Figure 15. Comparison of ground-level concentration on wake centerline with dispersion theory, ref. [20].